

Development of a vibratory source for shallow reverse VSP applications

Joe Wong and Robert R. Stewart

ABSTRACT

Shallow VSP surveys are useful for near-surface geotechnical applications and for obtaining data for statics corrections. When dense surface coverage is desired, VSP acquisition is much more efficient if it is done in the reverse configuration, i.e., with surface geophones and a downhole source. Considerations of safety and acquisition efficiency make it highly desirable to use a non-destructive, non-explosive downhole source for RVSP surveys. A suitable candidate for such a source is a vibrator controlled by frequency sweeps or pseudonoise sequences. In cooperation with JODEX Applied Geoscience Limited, the CREWES Project plans to adapt the CORRSEIS piezoelectric vibrator so that it can be used to conduct shallow RVSP surveys. The existing CORRSEIS vibrator produces seismic waves with dominant frequencies in the 2000 to 5000 Hz range. Such high frequencies are suitable for crosshole applications in high-Q rocks, but to be usable for RVSP where geophones are set on unconsolidated materials in the overburden, the vibrator must be redesigned to have dominant operating frequencies of 200 to 500 Hz. Other requirements are higher output power, and easy interfacing with recording instrumentation.

INTRODUCTION

Vertical seismic profiling (VSP) originated with check-shot shooting to obtain interval velocities critical for constructing depth sections from time sections. It has since evolved into a sophisticated method with wide application (Hardage, 1984; Toksoz and Stewart, 1984). VSP data have been used for imaging subsurface structure via VSP/CDP migration (Wyatt and Wyatt, 1984), converted-wave analysis of time-lapse 3C data (Coeslan et al., 2006), and estimation of Q in reservoir rocks (Haase and Stewart, 2006).

Conventional VSP acquisition is conducted with downhole sensors such as hydrophones and multi-component geophones placed at depth in a borehole and a source (dynamite or vibrator) on the surface. Areal coverage around the borehole results when many surface source locations are occupied. Mapping or migration of the multi-offset VSP data yields seismic depth images in a cone around the borehole. In many situations, dense surface coverage by source points is not possible due to restricted access by large vibrators or prohibited use of dynamite. Fewer access issues are connected with the placement of geophones on the surface, and data similar to normal VSP are obtained when a reversed configuration is used, i.e., with a downhole seismic source and surface geophones. It is much easier to deploy many geophones on the surface than it is to place many sensors in a borehole and, when high-density multi-component areal coverage is the goal, reverse VSP (RVSP) is much more efficient than conventional VSP simply because more channels can be recorded for each shot.

It is possible to use airguns and sparkers as downhole sources for RVSP (Howlett, 1991; Hardage, 1992). Blasting caps also have been employed for RVSP, and high quality data can be obtained because they generate good energy. However, they may damage boreholes, and they present issues of safety and reliability. Caps run a risk of being detonated accidentally during handling or not detonating at all when triggered. In addition, only a limited number of blasting caps can be put in a borehole at a time, and continually running loading cables up and down in order to occupy many source depths adversely affects field efficiency.

Controlled vibratory sources designed for downhole operation circumvent these issues. For example, Paulsson et al. (1997) have used a hydraulically-powered vertical vibrator in deep wells. Harris et al. (1995) reported applications where controlled sources based on piezoelectric technology were employed. Daley and Cox (2001) described an orbital vibrator, in which seismic energy is generated by rotating eccentric masses. These downhole sources are driven by frequency sweeps with energy in the 50 to 2000 Hz range. Alternatively, Wong et al. (1983) and Yamamoto et al. (1994) described downhole piezoelectric vibrators controlled by pseudo-random binary sequences (PRBS). In all cases, seismograms are obtained from vibrations detected by geophones or hydrophones by crosscorrelation with the pilot signal (a frequency sweep or pseudorandom sequence) controlling the source.

There are several important benefits when a controlled vibrator is used to obtain seismograms through crosscorrelation with a pilot signal:

1. Cross-correlation can enhance signal-to-noise ratios by a large factor that is dependent on the length and nature of the pilot.
2. Source power is distributed over time, and peak power can be kept low so that safety to operators and possibility of damage to boreholes are no longer issues.
3. Signals are highly repeatable because the source is controlled.
4. Summation of many identical waveforms (vertical stacking) during acquisition is straightforward, leading to further large increases in signal-to-noise ratios.

A downhole vibratory source draws power from electric or hydraulic pressure generators at ground level through multi-conductor cables or hydraulic lines. Once the controlled source is deployed in a deep well, it can be operated almost continuously without the need to return to the surface.

PILOT SIGNALS FOR CONTROLLING VIBRATORY SOURCES

Frequency Sweeps

A frequency sweep is a signal whose frequency changes monotonically with time. A linear sweep is defined by the equation

$$S_w = \sin (2\pi * [f_0 + (f_1-f_0) /T * t] * t) , \quad (1)$$

where f_0 and f_1 are the frequency limits of the sweep, T is the time duration of the sweep, and t is the time. If f_1 is greater than f_0 , then we have an upsweep (or chirp); if f_1 is less than f_0 we have a downsweep (or whistle). Figure 1a shows the initial 200 milliseconds of a linear upsweep with beginning frequency of 62.5 Hz, end frequency of 1000 Hz, and duration T of 512 milliseconds. Figure 1b is the sweep delayed by 20msec (representing the time a seismic signal takes to travel from a source to a detector). Figure 1c is the crosscorrelation of the delayed sweep with the original sweep. The delayed autocorrelation of the sweep is an approximation to a delayed delta function. Figure 1d is a seismic wavelet, and Figure 1e is the convolution of the wavelet with the delayed sweep. Figure 1f is the crosscorrelation of the signal 1e with the original sweep 1a, resulting in a version of the original wavelet arriving at the proper time. Note the coda in Figure 1f preceding the arrival time; this distortion of the original wavelet is due to the side lobes seen on the autocorrelation of the sweep. The distortion can be minimized to some extent if the bandwidth of the sweep is increased, especially at the low frequency end. Frequency sweeps need not be linear, but can be designed to emphasize different parts of the frequency range.

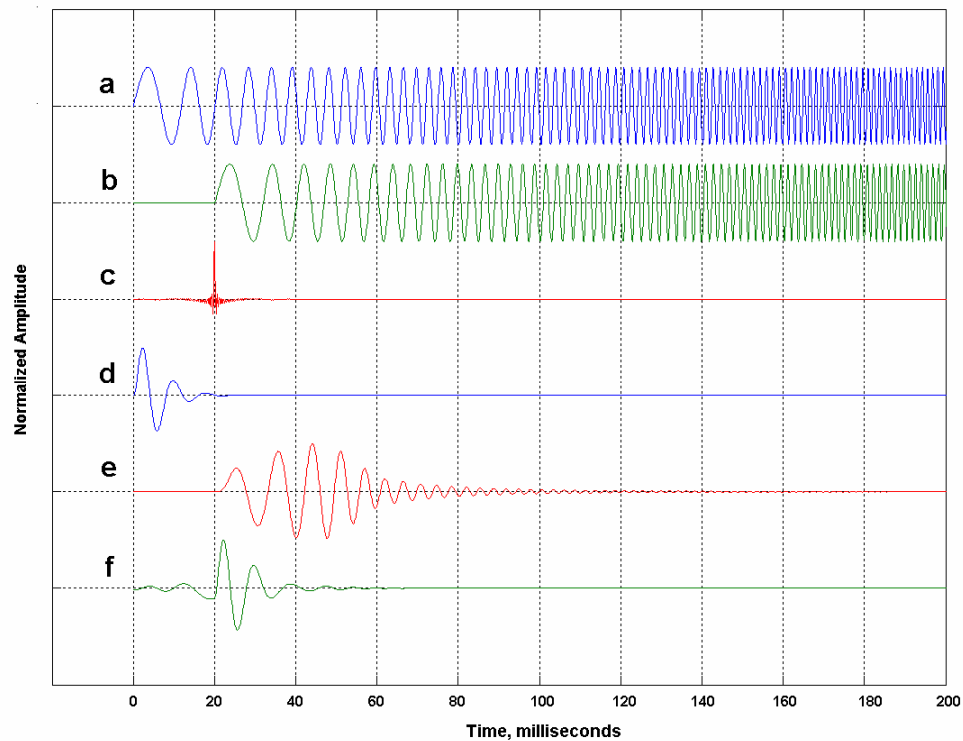


FIG. 1. (a) A linear frequency upsweep. (b) The sweep delayed by 20msec. (c) The crosscorrelation between the delayed sweep with the original sweep. (d) A seismic wavelet. (e) Convolution of the delayed sweep with the wavelet. (f) The crosscorrelation between the signal 1e and the original sweep 1a, giving a filtered, distorted version of the seismic wavelet arriving at a time of 20msec.

Maximal-Length PRBS

A PRBS is not so easily expressed by a simple formula such as Equation 1. However, a particular type called the maximal-length sequence or M-sequence (on which we will focus exclusively) is well-defined mathematically and is easily generated, both digitally, using logic statements, or electronically using simple circuits. A good summary on its properties is given on the website www.wikipedia.com under maximal length sequence.

The practical utility of an M-sequence PRBS lies in its simplicity and the nature of its autocorrelation. A particular sequence is a periodic stream of 1's and -1's, determined by its fundamental length L and its base period τ . The fundamental length L is given by the simple formula

$$L = (2^m - 1), \quad (2)$$

where m is a positive integer called the degree of the sequence. For example, pseudo-random M-sequences of lengths 31, 127, 2047, and 8191 are defined when m assumes the values 5, 7, 11, and 15. The base period τ is the shortest time between adjacent transitions in the sequence, while $T = L \cdot \tau$ is the period of the sequence. Electronic generation of a particular M-sequence requires a particular combination of shift registers and gates with unique feedback connections (Golomb, 1967).

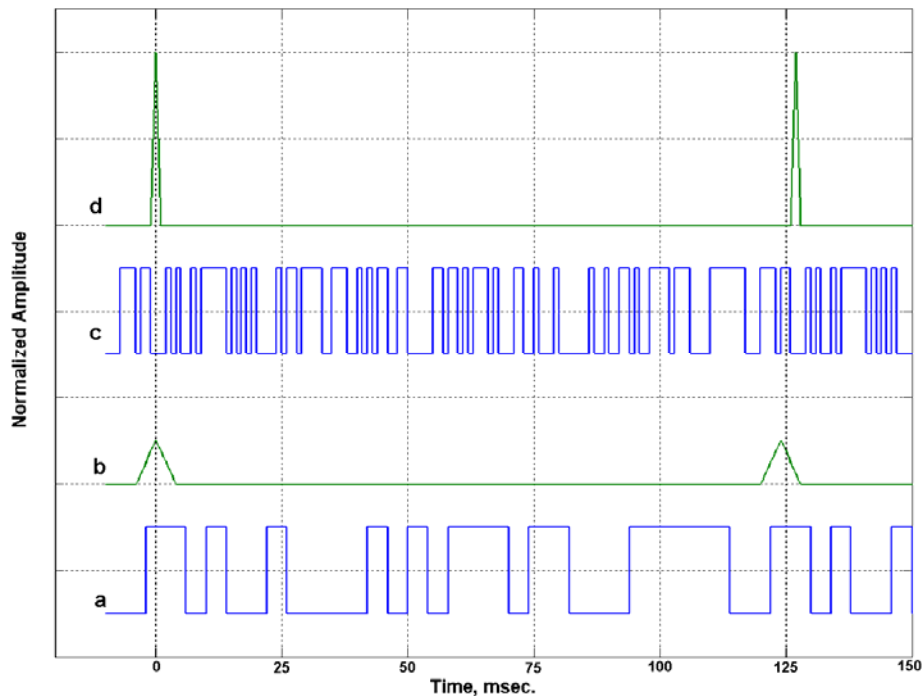


FIG. 2. (a) M-sequence PRBS with $L=31$ and $t=4\text{msec}$. (b) Autocorrelation of the sequence in Figure 1a. (c) M-sequence PRBS with $L=127$ and $t=1\text{msec}$. (d) Autocorrelation of the sequence in Figure 1c.

Figure 2a is an M-sequence PRBS with $L = 31$, $\tau = 4.0$ milliseconds, and $T = 124$ msec. Its autocorrelation, shown in Figure 2b, is a triangular spike with a peak proportional to L . The base of the triangle is 8msec, or $2*\tau$. If we scale the autocorrelation so that the peak has the value L (in this case, 31), then the autocorrelation peak will rest on a DC value of -1. That the ratio of the correlation peak to the DC value equals $(-L)$ will be true of any M-sequence.

Figure 2c is an M-sequence PRBS with $L=127$, $\tau=1$ msec, and period $T = 127$ msec. We see that its autocorrelation peak in Figure 2d is much sharper than that seen in Figure 2b. The scaled peak value is 127, while the base width of the correlation peak is 2msec. If we keep increasing the value of L by increasing m in Equation 2, while decreasing the base period τ (by a factor of 2 each time m changes by 1 so as to keep the sequence period T almost constant), the correlation peak becomes sharper and sharper, simulating a delta function better and better.

The power spectrum is discrete, with values at the discrete frequencies f_n given by the sinc-squared function:

$$S_n = \sin^2 (\pi * f_n / f_\tau) / (\pi * f_n / f_\tau)^2, \quad (3)$$

$$f_n = n * (f_\tau / L), \quad n = 1, 2, 3, \dots,$$

$$f_\tau = 1 / \tau.$$

The discrete power spectrum of the $L=127$ M-sequence (sampled at 0.25msec) is shown up to the Nyquist frequency in Figure 3.

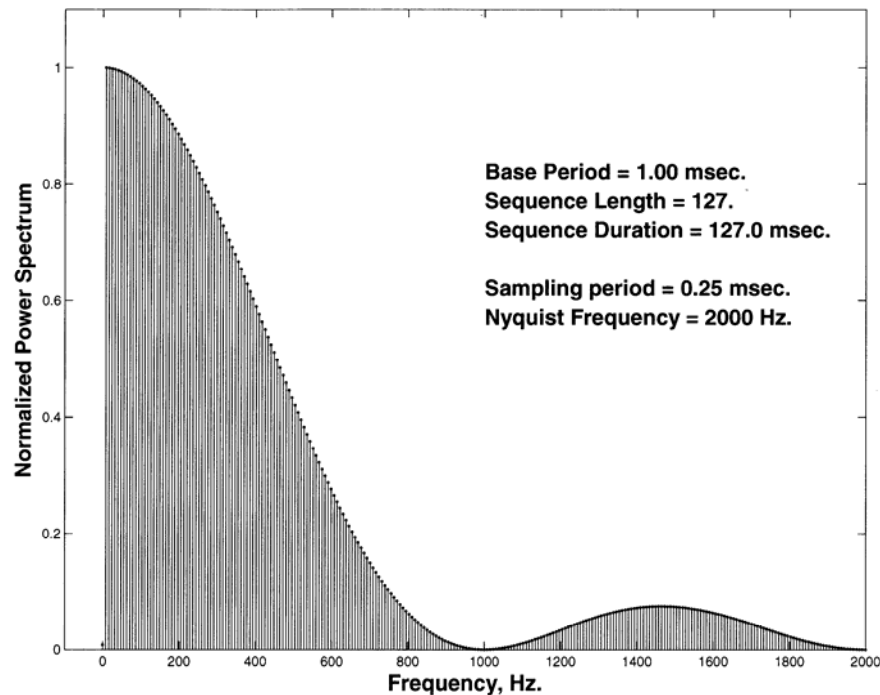


FIG. 3. Part of the power spectrum of the PRBS of Figure 1C.

The PRBS is sometimes referred to as a pseudonoise signal. One of the defining characteristics of a perfectly random signal or pure noise is that its autocorrelation is a delta function. Looking at the autocorrelation of the PRBS signal makes it clear how it simulates a pure noise signal. The sharp triangular peak becomes narrower in absolute time as τ is made smaller in absolute time, and its maximum value ($L*\tau = [2^m - 1]*\tau$) becomes larger as the sequence length increases, so that the PRBS behaves more and more like a true noise signal.

The well-behaved time and spectral characteristics of the PRBS have prompted numerous researchers to use it for analyzing linear systems (Engelberger and Benjamin, 2005). They have been incorporated into long-range radar and sonar applications where signal-to-noise enhancement is critical. For example, one of the first experiments in detecting radar echoes from Venus employed PRBS technology (Price et al., 1959). Behringer et al. (1982), and Birdsall et al. (1988) studied fluctuations in seawater acoustic velocities across thousands of kilometers with PRBS-coded sonar signals. Sachs et al. (2003) have described how modern short-range radar systems have adopted PRBS coding. Duncan et al. (1981) employed PRBS signals in a controlled source audio-frequency magnetotelluric (CSAMT) experiment. PRBS-coded piezoelectric vibrators have been used in borehole-to-borehole seismic surveys (Wong et al., 1983; Yamamoto, 1994; Wong, 2000).

SEISMIC ACQUISITION USING PRBS CROSSCORRELATION

Figure 4 shows the basic principles of using a PRBS in seismic data acquisition. A PRBS with fundamental length $L=127$, base period $t=1\text{msec}$ has been digitized with a sampling time of 0.25msec and plotted in Fig 4a. A phase-delayed version is shown on Figure 4b (remember that the PRBS is periodic, so that, in being delayed, its end wraps around to the beginning). The shift in the autocorrelation peaks on Figure 4c indicates that the delay is 40msec . Figure 4d is a seismic wavelet representing the impulse response (or transfer function) of a seismic source. When the source is driven by the undelayed PRBS, it generates a signature which is the convolution of the PRBS and the seismic wavelet. The signal propagates through the earth and is detected by a sensor some distance away.

The detected signal is represented by Figure 4e, which is the convolution of the PRBS and the wavelet, delayed by the traveltime. Figure 4f is the (circular) crosscorrelation of the detected signal with the undelayed PRBS, showing the seismic arrival as the original wavelet (with some filtering due to convolution and crosscorrelation with the PRBS) at a time exactly equal to the traveltime.

Figure 5 indicates the power of PRBS crosscorrelation in pulling weak signals out of strong random noise. Figure 5a is the seismic wavelet in Figure 4d with random background noise added. The signal-to-noise ratio (SNR), as determined by the short-term average squared amplitude of the wavelet to the mean-squared amplitude of the noise, is about 1. The important observation is that the noise completely obscures the wavelet. Figure 5b is the delayed convolution of Figure 4e, plus the same random noise. The SNR in Figure 5b appears to be higher than the SNR of Figure 5a because the mean

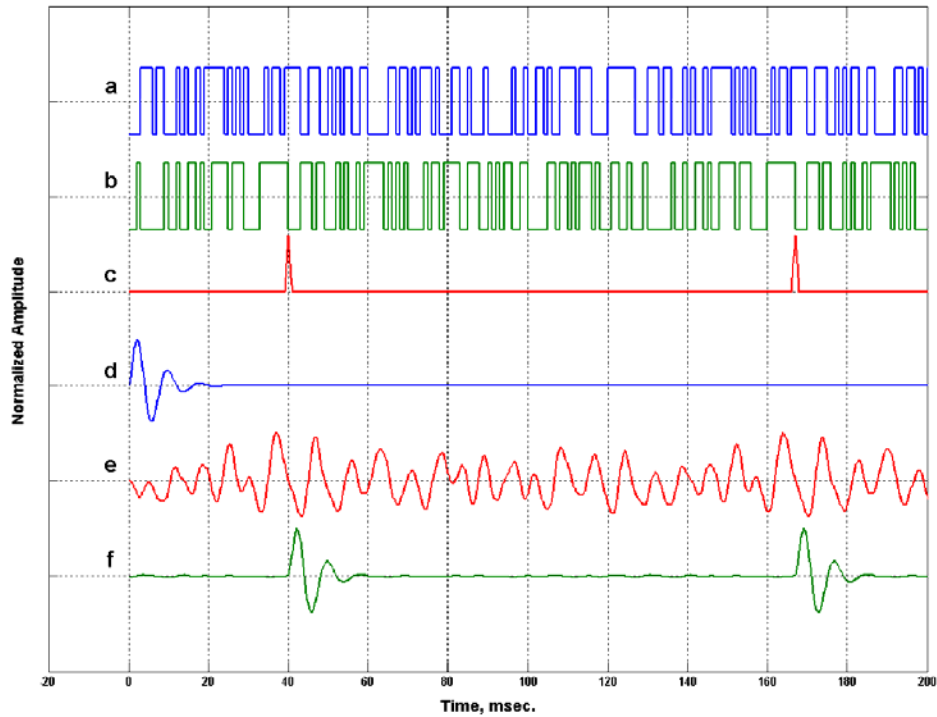


FIG. 4. (a) PRBS with $L=127$, $\tau=1$ msec. (b) PRBS of A delayed by 40msec. (c) The crosscorrelation between 4a and 4b. (d) A seismic wavelet. (e) The delayed PRBS convolved with the seismic wavelet. (f) The crosscorrelation of Figure 4e with the original PRBS in Figure 4a, recovering a filtered, periodic version of the original wavelet in Figure 4d.

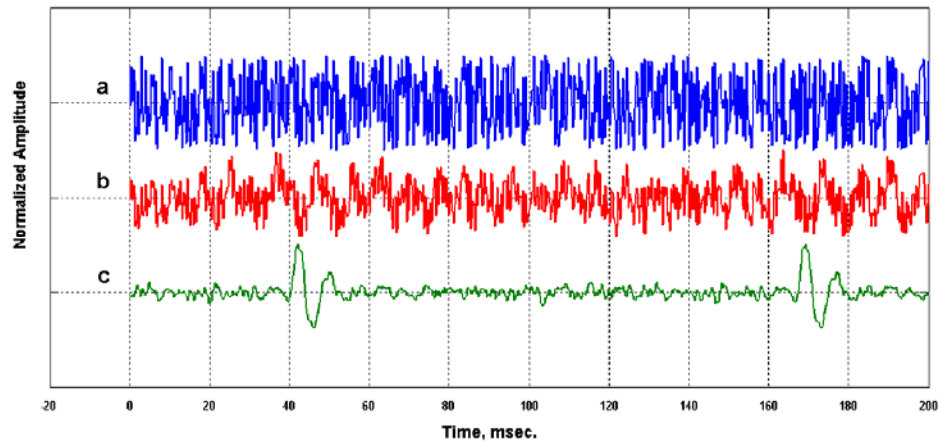


FIG. 5. Noise rejection feature of crosscorrelation. (a) The seismic wavelet of Figure 4d, plus random noise. (b) The convolved signal of Figure 4e, plus random noise. (c) The crosscorrelation of noisy signal of Figure 5b with the PRBS of Figure 4a.

squared amplitude of the convolved signal is somewhat larger than that of the wavelet by itself. Crosscorrelating the noisy detected signal with the PRBS pilot recovers the seismic arrival very effectively.

THE CORRSEIS PIEZOELECTRIC VIBRATOR

A vibratory seismic source can be controlled either by frequency sweeps or by pseudorandom sequences. The choice is based mostly on the particular application and the ease of matching the pilot signal to the mechanical features of the vibrator. Piezoelectric ceramic materials such as lead zirconate titanate are a good choice for generating seismic vibrations downhole. They are efficient transducers for converting time-varying electric voltages into mechanical vibrations.

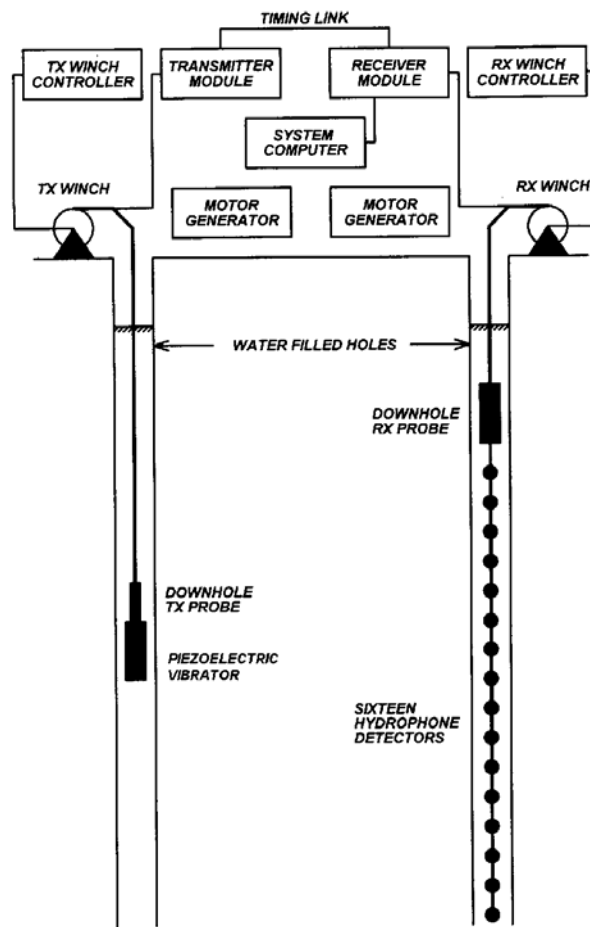


FIG. 6. CORRSEIS cross-borehole seismic system.

Figure 6 is a diagram of the CORRSEIS Borehole Seismic System developed by JODEX Applied Geoscience Limited. The system includes a piezoelectric vibrator as the downhole source, and is designed for high-resolution seismic scanning between holes separated by 10 to 100 meters. The instrumentation has been used extensively in igneous rock environments for orebody delineation in the mining industry, and between closely

spaced holes drilled in unconsolidated near-surface materials to support hydrogeological and geotechnical engineering activities.

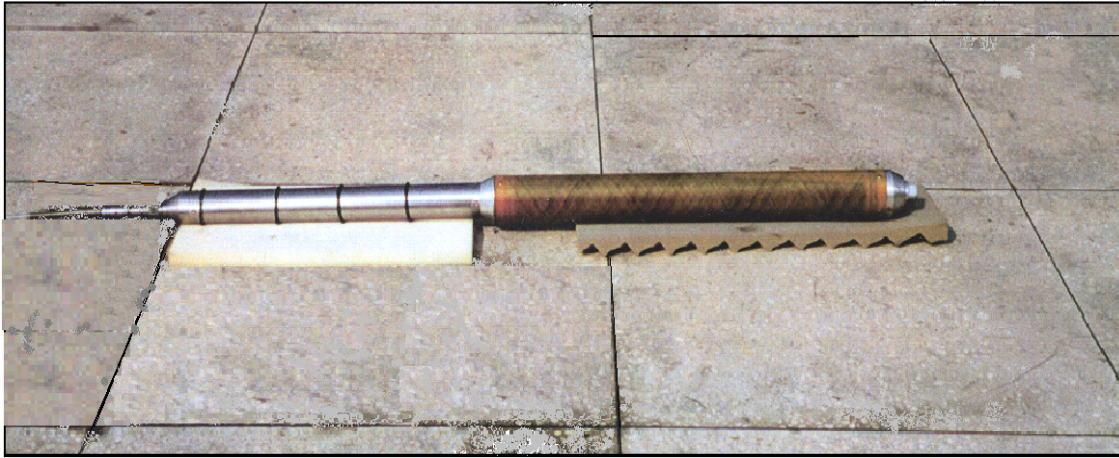


FIG. 7. CORRSEIS downhole piezoelectric vibrator.

The photograph of Figure 7 shows one version of the CORRSEIS piezoelectric vibrator. The upper stainless steel probe to the left contains the high voltage switching circuits that drive the piezoelectric ceramic transducers. The transducers themselves are housed in the lower, oil-filled fiberglass section to the right. These transducers are either small tubes, or small square plates stacked in parallel, formed and packaged to have mechanical resonances in the 2 to 5 kHz range. Their capacitances are resonated with series inductance to optimize the conversion of time-varying voltages to vibratory energy.

The vibrator can be driven by high-voltage frequency sweeps or M-sequences similar to that displayed on Figure 4A. In actual practice, the pilot is an M-sequence PRBS of degree $m=11$, i.e., of fundamental length $L=2047$. The base period used is 0.10msec, so that the first null in the power spectrum is at 10 kHz.

Figure 8 is common depth gather of crosscorrelation seismograms generated by the CORRSEIS vibrator operating in one borehole and recorded with hydrophone sensors in a second borehole about 80 meters away. The two boreholes were drilled in igneous rock and intersected a massive sulfide ore zone. The numbers in the columns under the TX and RX headings are the source and hydrophone depths in meters for the corresponding traces. For each trace, the source and hydrophone depths are almost the same; hence, the “common depth” appellation. We note that the dominant frequency in the traces is about 3 kHz. The first arrivals through the host rock come in at about 13msec, indicating a rock P-wave velocity of about 6200 m/sec. Through the sulfide zone, the latest arrival times are 16 to 17msec, indicating a P-wave velocity of about 4700 to 5000 m/sec.

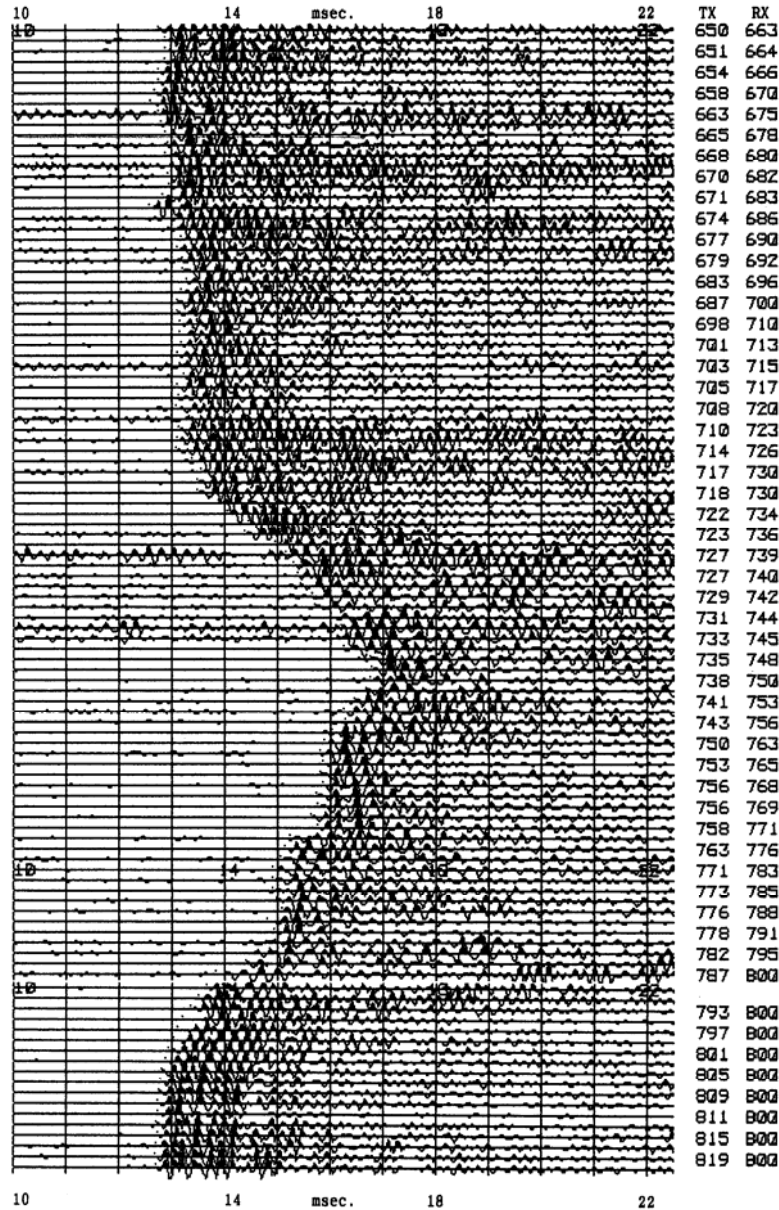


FIG. 8. A gather of crosshole seismograms recorded with hydrophones and the CORRSEIS vibrator source (courtesy of JODEX Limited). The numbers under the headings TX and RX are the source and hydrophone depths in meters.

A SOURCE FOR SHALLOW RVSP SURVEYS

We plan to employ the CORRSEIS vibrator for shallow RVSP surveys in holes up to 200 meters deep in overburden materials. As it exists, the CORRSEIS vibrator generates seismic waves with frequencies in the 2 to 5 kHz range, and its output power is rather modest (on the order of tens of watts). These frequencies are too high and the output power too low to be effective for propagation through any appreciable distance in

unconsolidated overburden materials. Therefore, to use the CORRSEIS vibrator for reverse vertical seismic profiling, we must modify its design and construction to:

1. lower the operating frequencies to the 200 to 500 Hz range;
2. increase the output power; and
3. interface with existing recording seismographs (e.g., the Geometrics R60).

The CREWES Project and JODEX Applied Geoscience Limited will cooperate to make these modifications to the original design. By the summer of 2007, the CREWES Project and the University of Calgary Department of Geology and Geophysics will have completed the drilling of a planned geophysical test hole (Wong et al., 2006), and we will conduct field trials of various enhanced versions of the vibrator using this test hole.

CONCLUSIONS

Reverse VSP in the shallow environment can be a valuable technique for acquiring seismic data to help solve the statics problem involving the overburden. Efficient RVSP field procedures require an effective and safe downhole source. Industry experience has confirmed that a controlled vibrator driven by a coded pilot signal such as a frequency sweep or pseudorandom sequence can serve very well as such a source. We have outlined how crosscorrelation methods, using a particular class of pseudorandom binary sequences (PRBS) known as M-sequences, are effective for seismic acquisition in low-signal/high-noise conditions. The CORRSEIS piezoelectric vibrator developed by JODEX Applied Geoscience Limited is a downhole source controlled by an M-sequence PRBS and designed for crosshole seismic scanning in high Q rocks. The CREWES Project will cooperate with JODEX Limited to modify the design so that it can be used as a source for reverse VSP surveys in shallow wells drilled in unconsolidated overburden materials.

ACKNOWLEDGEMENTS

We thank JODEX Applied Geoscience Limited for providing access to the design of the CORRSEIS piezoelectric vibrator.

REFERENCES

- Behringer, D., Birdsall, T., Brown, M., Cornuelle, B., Heinmiller, R., Knox, R., Metzger, K., Munk, W., Speisberger, J., Spindel, R., Webb, D., Worcester, P., and Wunsch, C., 1982, A demonstration of ocean acoustic tomography: *Nature*, **299**, 121-125.
- Birdsall, T.G., Metzger, K., and Spindel, R.C., 1988, Signal processing for ocean tomography with moving ships: *IEEE 22nd Asilomar Conf. on Signals, Systems, and Computers*, **1**, 436-439.
- Couelsan, M.L., Lawton, D.C., and Jones, M., 2006, Time-lapse monitoring of CO₂ EOR and storage with walkaway VSPs: 76th Annual International Meeting, SEG, Expanded Abstracts, 3130-3134.
- Daley, T.M., and Cox, D., 2001, Orbital vibrator for simultaneous P- and S-wave crosswell acquisition: *Geophysics*, **66**, 1471-1480.
- Duncan, P.M., Hwang, A., Edwards, R.N., Bailey, R.C., and G.D. Garland, 1980, The development and applications of a wide band electromagnetic sounding system using a pseudo-noise source, *Geophysics*, **45**, 1276-1296.

- Engelberg, S., and Benjamin, H., 2005, Pseudo-random sequences and the measurement of the frequency response: IEEE Instrumentation and Measurement Magazine, **8**, 54-59.
- Golomb, S., 1967, Shift register sequences: Holden-Day, San Francisco.
- Hardage, R.A., 1985, Vertical seismic profiling, part A-principles: 2nd Ed., Geophysical Press.
- Hardage, R.A., 1992, Crosshole seismology and reverse VSP: Geophysical Press.
- Haase, A., and Stewart, R.R., 2006, Intrinsic and apparent seismic attenuation in VSP data: 76th Annual International Meeting, SEG, Expanded Abstracts, 3472-3476.
- Harris, J.M., Nolen-Hoeksema, R.C., Langan, R.T., Van Schaak, M., Lazaratos, S.K., and Rector, J.W., 1995, High-resolution crosswell imaging of a west Texas carbonate reservoir: Part I-Project summary and interpretation: Geophysics, **60**, 667-681.
- Howlett, D.L., 1991, Comparison of borehole seismic sources under consistent field conditions: 61st Ann. Internat. Mtg., SEG, Expanded Abstracts, BG1.5, 18-19.
- Paulsson, B., Fairborn, J., and Fuller, B., 1997, Single well seismic imaging and reverse VSP applications for the downhole seismic vibrator: 67th ANN. Internat. Mtg., SEG, Expanded Abstracts, BH1.7, 246-247.
- Price, R., Green, P.E., Goblick, P.J., Kingston, R.H., Kraft, L.G., Pettengill, G.H., Silver, R., and Smith, W.B., 1959, Radar echoes from Venus: Science, **129**, 751-753.
- Sachs, J., Zetick, R., Peyerl, P., and Raushenbach, P., 2003, M-sequence ultra-wideband radar, state of development and applications: Proc. RADAR, Sept. 2-3, 2003, Adelaide, Australia.
- Toksoz, M.N., and Stewart, R.R., 1984, Vertical Seismic Profiling, Part B, Advanced Concepts, Geophysical Press.
- Wong, J., Lawton, D.C., Bertram, M.B., and Stewart, R.R., 2006, Current and planned VSP capabilities within CREWES: CREWES Research Reports, this volume.
- Wong, J., Hurley, P., and West, G.F., 1983, Crosshole seismology in crystalline rocks: Geophys. Res. Lett., **10**, 686-689.
- Wong, J., 2005, Crosshole seismic imaging for sulfide orebody delineation near Sudbury, Ontario, Canada: Geophysics, **65**, 1900-1907.
- Wyatt, K.D., and Wyatt, S.B., 1984, Subsurface structure using the vertical seismic profile, *in* Toksoz, M.N., and Stewart, R.R., Eds., Vertical seismic profiling, part B, advanced concepts, Geophysical Press
- Yamamoto, T., Nye, T., Kuru, M., 1994, Porosity, permeability, shear strength: crosswell tomography beneath an iron foundry: Geophysics, **59**, 1530-1541.